Optimal Scheduling of EV Charging Stations with Integrated Renewable Resources Using the Mantis Search Algorithm

Khoa Hoang Truong
Department of Power Delivery, Ho Chi Minh City University of Technology (HCMUT), Dien Hong Ward, Ho Chi Minh City, Vietnam | Vietnam National University Ho Chi Minh, Linh Xuan Ward, Ho Chi Minh City, Vietnam
trhkhoa@hcmut.edu.vn

Hung Duc Nguyen
Department of Power Delivery, Ho Chi Minh City University of Technology (HCMUT), Dien Hong Ward, Ho Chi Minh City, Vietnam | Vietnam National University Ho Chi Minh, Linh Xuan Ward, Ho Chi Minh City, Vietnam
hungnd@hcmut.edu.vn

Dieu Ngoc Vo
Department of Power Systems, Ho Chi Minh City University of Technology (HCMUT), Dien Hong Ward, Ho Chi Minh City, Vietnam | Vietnam National University Ho Chi Minh, Linh Xuan Ward, Ho Chi Minh City, Vietnam
vndieu@hcmut.edu.vn (corresponding author)

Received: 21 September 2025 | Revised: 4 November 2025 and 26 November 2025 | Accepted: 28 November 2025

 DOI: https://doi.org/10.48084/etasr.14981

ABSTRACT

The transportation sector is rapidly transitioning toward carbon neutrality through the large-scale deployment of Electric Vehicles (EVs), which necessitates efficient and sustainable Charging Station (CS) infrastructures. This study develops a comprehensive CS model that integrates Renewable Energy Sources (RESs), Energy Storage Systems (ESSs), and the utility grid to meet EV demands while enhancing energy flexibility and sustainability. A novel Mantis Search Algorithm (MSA) is employed for operational scheduling with a profit-maximization objective. The MSA features a robust exploitation operator that improves convergence and effectively avoids local optima in unimodal optimization problems. Extensive evaluations were conducted across multiple scenarios: CSs without ESS, with ESS without export capability, and the proposed integrated model. The results demonstrate that the comprehensive configuration improves system performance by 10.35% and 21.99% compared to the two baseline cases. Furthermore, the proposed MSA demonstrates significantly better performance than other compared methods, highlighting its effectiveness in optimizing energy management in CSs. These results demonstrate the promising potential of the MSA-based day-ahead schedule to support resilient, cost-effective, and environmentally sustainable CSs.

Keywords-charging station; electric vehicles; energy storage systems

I. INTRODUCTION

Transportation is essential for both society and the economy, accounting for approximately 35% of total energy consumption. This sector contributes significantly to greenhouse gas emissions and air pollution due to fossil fuel use (mainly diesel). Collaborative efforts among governments, businesses, and individuals are critical to reducing emissions and optimizing energy efficiency. Electrification is an effective solution promoted by many countries to reduce their dependence on fossil fuels in transportation and cut carbon emissions. The incorporation of EV loads into power grids has substantially intensified network energy demand, requiring the implementation of a modern self-regulated grid. In addition, integrating ESS and RES into Charging Stations (CS) affects the operation and performance of the Distribution Network (DN). Therefore, developing an optimal scheduling approach for CS is essential.

Research focuses on coordinated EV charging strategies aimed at minimizing charging costs, mitigating voltage deviations, reducing peak load demand, ensuring system reliability, and alleviating overloading at CSs. In [1], optimal strategies for deploying CS infrastructure and common standards to address integration issues were identified. Authors in [2] presented a mathematical model for optimizing the operation scheduling of a remote PV farm and CS. Authors in [3] introduced a novel Energy Management Strategy (EMS) for a residential CS powered by PV energy, which is grid-connected and equipped with an ESS sized according to residential parking patterns. In [4], an optimal sizing framework was proposed for the CSs, addressing increased peak loads and component overloading due to PV-EV integration. Authors in [5] utilized simultaneous Particle Swarm Optimization (PSO) on IEEE 15, 33, 69, and 85 bus systems. Authors in [6] proposed an opposition-based competitive swarm optimization for optimal charge/discharge scheduling of EVs at CSs. Authors in [7] proposed a dynamic pricing strategy for CSs to increase profits while mitigating the negative impacts of EV proliferation on the DN and transportation networks. In [8], a hybrid Grey Wolf Optimization (GWO) and Dynamic Fitness-Distance Balance was proposed to optimize CS operation, aiming to minimize voltage deviations and active power losses. In [9], a battery-independent power conversion system model was introduced for optimizing ESS and PV capacities in a CS to maximize profits. Authors in [10] proposed a model to optimize EV fleet charging using photovoltaic-storage-CSs and the electricity grid. Authors in [11] introduced an enhanced capuchin search for simultaneously allocating CSs and RES in a smart grid. In [12], a two-stage strategy was presented for planning the integration of CSs and renewable DGs, including PV and Wind Turbines (WT). Other metaheuristics have been applied to optimization problems, such as the equilibrium optimizer [13] and symbiotic organisms search [14].

Although EVs have been recognized as sustainable transportation solutions, insufficient attention has been given to the environmental impact and emission-reduction potential of integrating CSs with ESS and grid-connected RES. The present research addresses these gaps by incorporating environmental objectives into the energy-management strategy and proposing a comprehensive optimization framework. This framework enhances scheduling flexibility for coordinated RES–CS operation by effectively combining the utility grid, RES, and ESS to meet EV demand. The multi-source configuration enhances energy flexibility, maximizes RES utilization, and provides a more reliable and sustainable charging infrastructure for EVs. An MSA is applied to optimize the scheduling of a CS with integrated BESS and RES, connected to the utility grid, aiming to find an optimal balance between profit and emission costs. The proposed EMS strategy is shown to be superior to the Slime Mould Algorithm (SMA), Harris Hawk Optimizer (HHO), and Hunger Games Search (HGS) methodologies effectively. Thus, the results of the current work confirm that the proposed MSA effectively optimizes energy management for CSs.

II. PROBLEM FORMULATION

This study proposes a CS model that is connected to the utility grid, PV, WT, and BESS, as shown in Figure 1.

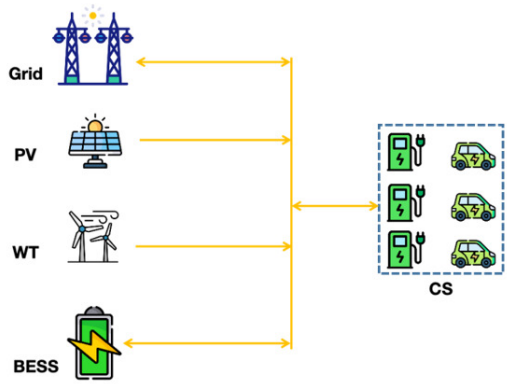

Fig. 1. CSs model with multiple power sources.

A. Charging Stations

The proposed CS effectively manages the charging and discharging schedules of a large fleet of EVs:

$$\sum_{t_a^n}^{t_d^n} e^n(t) = \begin{cases} e^n(t-1) + \dfrac{P_{EV}^n(t)}{C_{EV}} \cdot \eta_{EV,ch} \cdot \Delta t, & P_{EV}^n(t) \geq 0 \\ e^n(t-1) + \dfrac{P_{EV}^n(t)}{C_{EV} \cdot \eta_{EV,dch}} \cdot \Delta t, & P_{EV}^n(t) < 0 \end{cases} \quad (1)$$

$$-P_{EV,dch}^{\max}(t) \leq P_{EV}^n(t) \leq P_{EV,ch}^{\max} \quad (2)$$

$$e^{\min} \leq e^n(t) \leq e^{\max} \quad (3)$$

The SOC of EVs is calculated based on the arrival time (t_a^n), departure time (t_d^n), charging efficiency ($\eta_{EV,ch}$), discharging efficiency ($\eta_{EV,dch}$), and EV battery capacity (C_{EV}). Each EV operates within maximum charging ($P_{EV,ch}^{max}$) and discharging ($P_{EV,dch}^{max}$) power, as demonstrated in (2). In (3), the SOC has to remain within a range between e^{min} and e^{max}.

The profit cost of CS is expressed by:

$$\text{Pro}_{CS}(t) = \sum_{n=1}^{N} \begin{cases} P_{EV}^n(t) \cdot \pi_{ch,EV}(t) \cdot \Delta t, & P_{EV}^n(t) \geq 0 \text{ (charge)} \\ P_{EV}^n(t) \cdot \pi_{dch,EV}(t) \cdot \Delta t, & P_{EV}^n(t) < 0 \text{ (discharge)} \end{cases} \quad (4)$$

$$Pen_{CS}(t) = \sum_{n=1}^{N} (SOC_{des}^n - SOC^n(t_d^n)) \cdot \pi_{pen} \cdot \Delta t \quad (5)$$

where the profit of the CS for each interval time ($Pro_{CS}(t)$) is calculated based on electricity transactions, where the station earns from charging EVs at price $\pi_{ch,EV}$, and pays EVs for discharged energy at price $\pi_{dch,EV}$. Through (5), the CS is penalized if an EV departs with an SOC that does not meet its desired value (SOC_{des}^n), where π_{pen} indicates the penalty cost.

B. Battery Energy Storage Systems

The operational constraints of BESS are:

$$E_{BESS}(t) = \begin{cases} P_{BESS}(t-1) + P_{BESS}(t) \cdot \eta_{BESS,ch} \cdot \Delta t, & P_{BESS}(t) \geq 0 \text{ (charge)} \\ P_{BESS}(t-1) \cdot \dfrac{P_{BESS}(t)}{\eta_{BESS,dch}} \Delta t, & P_{BESS}(t) < 0 \text{ (discharge)} \end{cases} \quad (6)$$

$$-P^{\max}_{BESS,dch}(t) \leq P_{BESS}(t) \leq P^{\max}_{BESS,ch} \quad (7)$$

$$E^{\min}_{BESS} \leq E_{BESS}(t) \leq E^{\max}_{BESS} \quad (8)$$

$$E_{BESS}(0) = E_{BESS}(T) \quad (9)$$

The power level of BESS ($E_{\mathrm{BESS}}(t)$) at each interval time is defined in (6). Here, $P_{\mathrm{BESS}}(t)$ is the charging/discharging power of the BESS at time t, bounded between the maximum charging power ($P^{max}_{\mathrm{BESS,ch}}$) and maximum discharging power ($P^{max}_{\mathrm{BESS,dch}}$). Furthermore, the charging and discharging efficiencies are given by $\eta_{\mathrm{BESS,ch}}$ and $\eta_{\mathrm{BESS,dch}}$, respectively. Constraint (8) ensures that the energy level stays within the minimum (E^{min}_{BESS}) and maximum (E^{max}_{BESS}) storage capacity limits. Finally, (9) ensures that the energy at the beginning and the end of the horizon T remains equal.

C. Photovoltaic Panels

In this system, PV output is computed by:

$$P_{PV}(t) = G(t) \cdot \eta_{PV} \cdot \bar{P}_{PV} \cdot \Delta t \quad (10)$$

where the PV output ($P_{PV}(t)$) is computed based on solar irradiance ($G(t)$), PV efficiency (η_{PV}), and PV rated power capacity ($\bar{P}_{\mathrm{PV}}$).

D. Wind Turbines

In this system, WT output is computed using:

$$P_{WT}(t) = \begin{cases} 0; & if\, v(t) \leq v^{ci} \\ \dfrac{v(t)-v^{ci}}{v^{r}-v^{ci}} \cdot P^{r}; & if\, v^{ci} < v(t) \leq v^{r} \\ P^{r}; & if\, v^{r} < v(t) \leq v^{co} \\ 0; & if\, v(t) > v^{co} \end{cases} \quad (11)$$

where the WT output ($P_{\mathrm{WT}}(t)$) is determined by the current, cut-in, rated, and cut-out wind speeds ($v(t), v^{\mathrm{ci}}, v^{r}, v^{\mathrm{co}}$) and the rated output ($P^{r}$).

E. Energy Balance

During the CS operation, the balance must be followed:

$$P_{Grid}(t) = P_{WT}(t) + P_{PV}(t) + P_{BESS}(t) + \sum_{n=1}^{N} P^{n}_{EV}(t) \quad (12)$$

where $P_{Grid}(t)$ indicates the grid electricity.

The fitness function for the CS accounts for grid costs, CS operating costs, and penalty costs:

$$FF = \sum_{t=1}^{T} (P_{Grid}(t)\pi_{Grid}(t) + Pen_{CS}(t) - Pro_{CS}(t)) \quad (13)$$

where $\pi_{Grid}(t)$ is the electricity cost at time t.

III. MANTIS SEARCH OPTIMIZATION ALGORITHM

A. Initial Population

The MSA generates an initial population using:

$$\vec{x}_i^{\,t} = \vec{x}^{L} + \vec{R} * (\vec{x}^{U} - \vec{x}^{L}) \quad (14)$$

where $\vec{x}^{L}$ and $\vec{x}^{U}$ denote the vectors of lower and upper bounds for each j-dimension, respectively. In this study, $\vec{R}$, R_1, R_2, R_3, $\vec{R}_4$, $\vec{R}_5$, R_6, R_7, $\vec{R}_8$, R_9, R_{10}, $\vec{R}_{16}$, R_{17}, and $\vec{R}_{18}$ are randomly generated vectors/numbers in the range [0, 1].

B. Search for Prey: Exploration Stage

The proposed method integrates both Lévy flight and normal distribution techniques using:

$$x_i^{t+1} = \begin{cases} x_i^t + \tau_1 * (x_i^t - x_X^t) + |\tau_2| \cdot \vec{U} * (x_X^t - x_Y^t), & R_1 < R_2 \\ x_i^t * \vec{U} + (x_X^t + R_3 * (x_Y^t - x_Z^t)) * (1 - \vec{U}), & \text{otherwise} \end{cases} \quad (15)$$

where x_i^t denotes the position of the i^{th} mantis at the function evaluation step t. The symbol * represents the Hadamard (element-wise) product between vectors, while · refers to standard scalar multiplication. The vector τ_1 is generated using the Lévy flight mechanism, and τ_2 is a random scalar drawn from a normal distribution. The vectors x_X^t, x_Y^t, and x_Z^t are randomly chosen solutions from the current population. $\vec{U}$ is a binary mask vector computed using:

$$\vec{U} = \begin{cases} 0, & \vec{R}_4 < \vec{R}_5 \\ 1, & \text{otherwise} \end{cases} \quad (16)$$

where for each dimension j, the corresponding element in $\vec{R}_4$ is compared with that in $\vec{R}_5$. The ambush mantis remains motionless and effectively camouflaged using:

$$\vec{x}_i^{t+1} = \vec{x}_i^t + a \cdot (\vec{x}_{rand'} - \vec{x}_X^t) \quad (17)$$

where $\vec{x}_{rand'}$ is a randomly selected solution from the archive. Scaling factor α is defined as:

$$a = \cos(\pi \cdot R_6) \cdot \mu \quad (18)$$

where μ is a distance factor and computed by:

$$\mu = \left(1 - \frac{t}{T}\right) \quad (19)$$

where T denotes the maximum number of function evaluations. The prey actively searches for food using:

$$\vec{x}_i^{t+1} = \vec{x}_{rand'} + (R_7 \cdot 2 - 1) \cdot \mu \cdot (\vec{x}^{L} + \vec{R}_8 \cdot (\vec{x}^{U} - \vec{x}^{L})) \quad (20)$$

As iterations proceed, the distance gradually decreases as:

$$\vec{x}_i^{t+1} = \begin{cases} \vec{x}_i^t + \alpha \cdot (\vec{x}_{rand'} - \vec{x}_X^t), & R_9 \leq R_{10} \\ \vec{x}_{rand'} + (R_7 \cdot 2 - 1) \cdot \mu \cdot (\vec{x}^{L} + \vec{R}_8 \cdot (\vec{x}^{U} - \vec{x}^{L})), & \text{otherwise} \end{cases} \quad (21)$$

The formula for the cycling control factor is expressed as:

$$F = 1 - \frac{t\%(T/P)}{T/P} \quad (22)$$

where the symbol % denotes the remainder (modulus) operator and the variable P is an integer that indicates the number of cycles.

C. Attacking the Prey: Exploitation Stage

Targeted motion motivates an efficient exploration mechanism in optimization using:

$$V_{str} = \frac{1}{1+e^{\rho \cdot Rate}} \quad (23)$$

where V_{str} denotes the strike velocity, and ρ is a constant defining the gravitational acceleration of the mantis's strike. The value Rate is randomly selected between -2 and -1. Each position of the mantis is updated using:

$$x_{i,j}^{t+1} = \frac{(x_{i,j}^{t} + x_j^{*})}{2} + V_{str} \cdot D_{i,j}^{t} \quad (24)$$

where $x_{i,j}^{t}$ is the current position of the i^{th} mantis in the j^{th} dimension, x_j^{*} is the best position, and $D_{i,j}^{t}$ is the distance of the strike in iteration t.

In the proposed algorithm, $D_{i,j}^{t}$ is computed by:

$$D_{i,j}^{t} = (x_j^{*} - x_{i,j}^{t}) \quad (25)$$

The new direction is computed by:

$$x_{i,j}^{t+1} = x_{i,j}^{t} + R_{12} \cdot (x_{X,j}^{t} - x_{Y,j}^{t}) \quad (26)$$

where $x_{X,j}^{t}$ and $x_{Y,j}^{t}$ are randomly selected mantises from the current population, scaled by a random factor $R_{12} \in (0,1)$.

An update mechanism is proposed to escape local optimum:

$$x_{i,j}^{t+1} = x_{i,j}^{t} + e^{2 \cdot Rate} \cdot \cos(2 \cdot \pi \cdot Rate) \cdot \left| x_{i,j}^{t} - x_{rand,j}^{'t} \right| + (2 \cdot R_{13} - 1) \cdot (x_j^{u} - x_j^{Rate}) \quad (27)$$

A failure probability is used:

$$P_{fail} = a \cdot \left(1 - \frac{t}{T}\right) \quad (28)$$

where a is a constant, t is the current function evaluation, and T is the maximum number of function evaluations.

D. Sexual Cannibalism

The mate attraction process can be modeled using:

$$\vec{x}_i^{t+1} = \vec{x}_i^{t} + \vec{R}_{16} * (\vec{x}_i^{t} - \vec{x}_X^{t}) \quad (29)$$

where $\vec{x}_i^{t+1}$ is the position of a female praying mantis, while $\vec{x}_X^{t}$ is a randomly selected solution from the population that represents a male drawn to the female for mating, after which he may be consumed.

In general, the probability of mate attraction in the generation t, denoted as P_{ma}, is mathematically defined as:

$$P_{ma} = R_{17} \cdot \mu \quad (30)$$

This process is mathematically formulated as:

$$\vec{x}_i^{t+1} = \vec{x}_i^{t} * \vec{U} + (x_{11}^{t} + \vec{R}_{18} * \left(-x_{11}^{t} + \vec{x}_i^{t}\right)) * (1 - \vec{U}) \quad (31)$$

where x_{11}^{t} is the value of the first dimension of the first mantis.

During or following the mating process, a behavior is modeled mathematically by:

$$\vec{x}_i^{t+1} = \vec{x}_a^{t} \cdot \cos(2\pi l) \cdot \mu \quad (32)$$

where $\vec{x}_a^{t}$ represents the male and μ is the eaten part from the male. The MSA flowchart is presented in Figure 2.

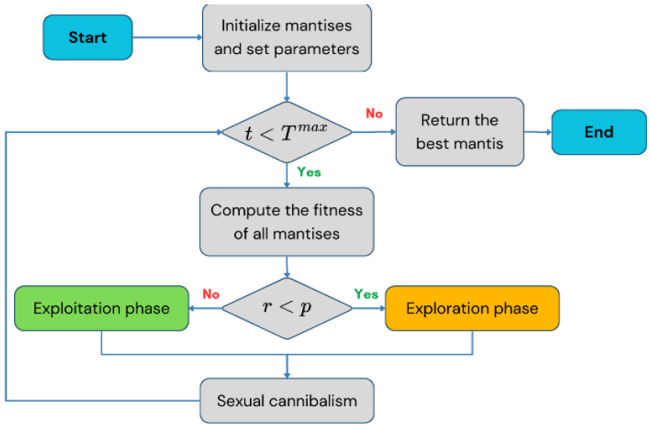

Fig. 2. Flowchart of the MSA.

IV. RESULTS

A. Data Description

To evaluate the proposed method, a CS with RES and the grid price is evaluated. Table I presents the parameters of EV and BESS. Furthermore, the RES power is scaled to match the requirements of the proposed model, as illustrated in Figure 3.

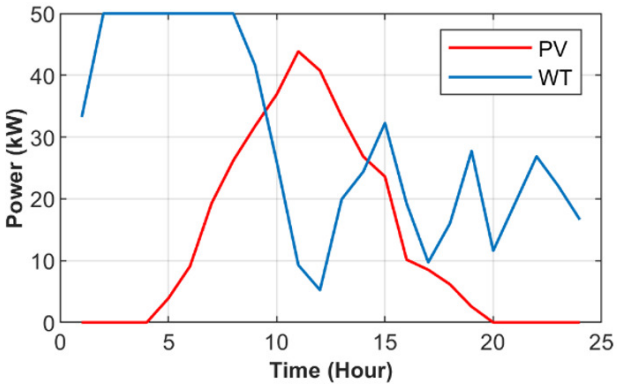

Fig. 3. PV and WT output power.

TABLE I. PARAMETERS OF EV AND BESS

Parameters	Value
Number of EVs (N)	10
Charging efficiency of EVs ($\eta_{EV,ch}$)	0.9
Discharging efficiency of EVs ($\eta_{EV,dch}$)	0.9
Minimum SOC of EVs (SOC^{min})	0.3
Maximum SOC of EVs (SOC^{max})	0.9
Maximum charging power of EVs ($P_{EV,ch}^{max}$)	50 kW
Minimum discharging power of EVs ($P_{EV,dch}^{max}$)	50 kW
Battery capacity of EVs (C_{EV})	200 kWh
Penalty price (π_{pen})	$ 1
Charging efficiency of BESS ($\eta_{EV,ch}$)	0.9
Discharging efficiency of BESS ($\eta_{EV,dch}$)	0.9
Minimum BESS capacity (E_{BESS}^{min})	100 kWh
Maximum BESS capacity (E_{BESS}^{max})	500 kWh
Maximum charging power of BESS ($P_{BESS,ch}^{max}$)	100 kW
Minimum discharging power of BESS ($P_{BESS,dch}^{max}$)	100 kW

TABLE II. RESULTS OF THREE CASES

	Grid cost ($)	Profit from grid ($)	Profit from EVs ($)	Total profit ($)
Case 1	402.06	256.63	509.66	364.23
Case 2	125.34	0	446.22	320.88
Case 3	342.42	342.86	456.66	457.1

B. Case Studies

Three cases are examined:

- Case 1: The system operated without a BESS. The CS can both buy and sell electricity to the grid.
- Case 2: The system is integrated with BESS. The CS can only buy electricity from the grid (no selling allowed).
- Case 3: The system is integrated with BESS. The CS can both buy and sell electricity to the grid.

Table II presents the results of the three different cases in terms of grid cost, profit from the grid, and profit from EVs. Case 3 is the most profitable, achieving the highest total profit of $457.1. This model operates with a BESS and gains profit from the grid. Although Case 1 incurs the highest grid cost ($402.06), it also achieves the highest EV profit of $509.66. In contrast, Case 2, which has the lowest grid costs ($125.34), yields the lowest total profit ($320.88). This highlights the importance of balancing grid transactions and BESS operation to maximize total profitability.

1. Case 1

The CS exhibits high power demand during high-price hours (hours 11-14), as illustrated in Figures 4 and 5. Meeting this demand with electricity from the grid is the main reason for the high grid cost. The surplus power is fully sold to the grid.

2. Case 2

In case 2, the model avoids buying electricity during peak hours. The BESS charges during low-price hours (hours 0-4) and discharges during high-price hours (hours 9-19). The surplus electricity from RES, along with power discharging from EVs, is stored in BESS for peak hours, as shown in Figures 6 and 8. Therefore, with BESS integration, the grid cost is reduced. However, the inability to export excess energy to the grid prevents full utilization of surplus generation, which limits the overall profit potential.

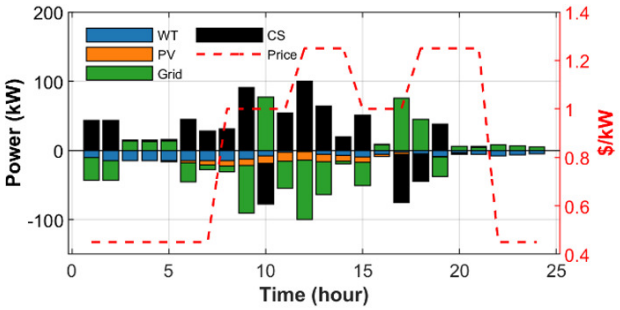

Fig. 4. Electricity profile for Case 1.

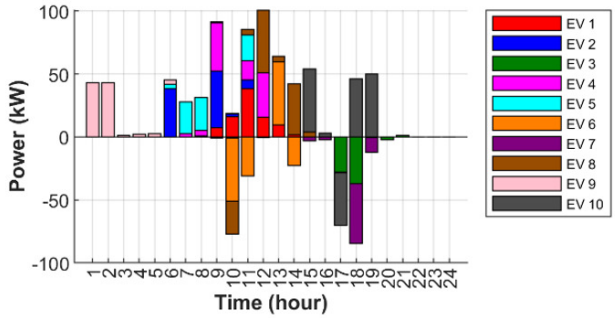

Fig. 5. EV charging/discharging power in Case 1.

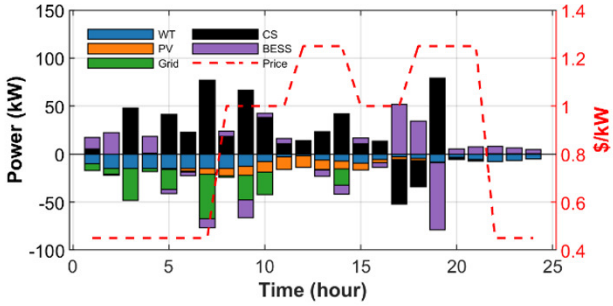

Fig. 6. Electricity profile for Case 2.

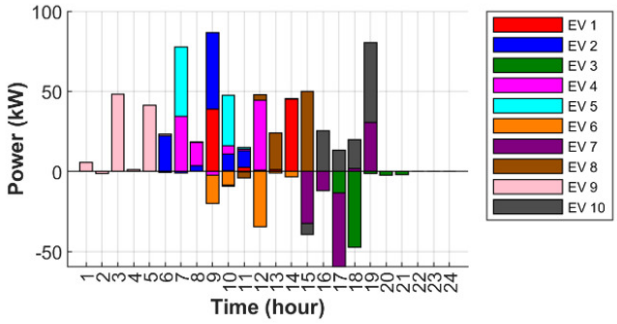

Fig. 7. EV charging/discharging power in Case 2.

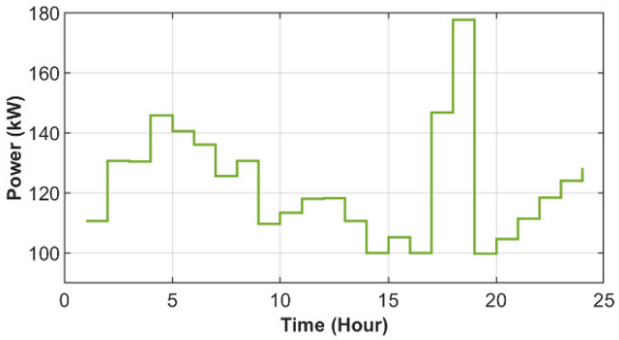

Fig. 8. BESS capacity in Case 2.

3. Case 3

In case 3, the BESS operates on a strategy: it charges when grid prices are low and discharges during high-price periods (Figure 11). Furthermore, surplus energy from RES and EV discharging power are also preferred to be stored in BESS for backup or export at peak hours (Figure 9). While this approach to reducing grid costs is similar to Case 2, Case 3 has the additional capability to sell surplus energy to the grid in the high-price period, in order to increase the profit from the grid. This results in the highest total profit among all cases, as displayed in Table II.

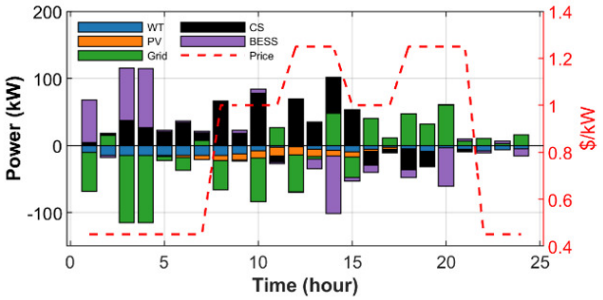

Fig. 9. Electricity profile for Case 3.

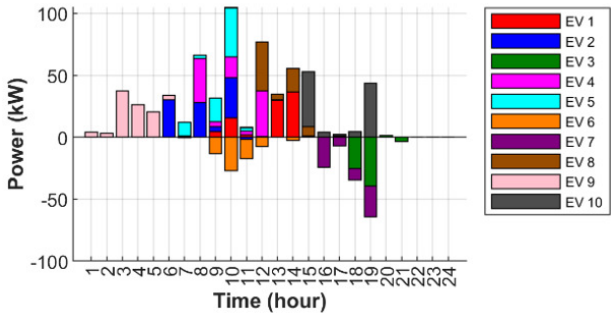

Fig. 10. EV charging/discharging power in Case 3.

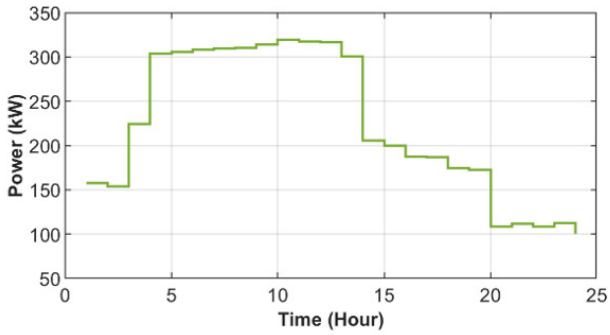

Fig. 11. BESS capacity in Case 3.

C. Comparison with Other Methods

Table III presents a comparative analysis of the proposed method, MSA, with SMA, HHO, and HGS. All algorithms are executed for 10 independent runs, with a population size of 100, and a maximum of 10,000 generations. MSA achieves the highest total profit ($457.10). This algorithm also yields the highest EV profit ($456.66) and grid profit ($342.86). In contrast, HHO records the lowest total profit ($318.10). Overall, MSA demonstrates the optimal solution.

TABLE III. COMPARATIVE ANALYSIS OF EXISTING LITERATURE AND PROPOSED TECHNIQUE

	Grid cost ($)	**Profit from grid ($)**	**Profit from EVs ($)**	**Total profit ($)**
SMA	308.07	246.31	408.76	346.99
HHO	279.72	253.46	344.36	318.1
HGS	326.86	254.31	424.33	351.78
MSA	342.42	342.86	456.66	457.1

V. CONCLUSIONS

This research investigates the optimal scheduling of Charging Stations (CSs) that integrate BESSs and Renewable Energy Sources (RES).

The objective of the problem is to maximize operational profit, reduce energy costs, enhance the utilization of renewable energy, and maintain energy balance within the system. Across three study cases, the comprehensive case delivers the most favorable outcome, improving overall performance by 20.35% relative to the no BESS integration and by 30% relative to the no electricity export. Moreover, MSA yields the best total profit ($457.10), outperforming the Slime Mould Algorithm (SMA, $346.99), Hunger Games Search (HGS, $351.78), and Harris Hawk Optimizer (HHO, $318.10). This performance gap underscores MSA's ability to exploit arbitrage opportunities without premature convergence. Operationally, the findings suggest that BESS flexibility should be co-optimized with bilateral grid transactions to efficiently serve Electric Vehicle (EV) demand. Future work will focus on extending the model to incorporate real-time demand response and dynamic pricing mechanisms, thereby further enhancing scheduling flexibility and economic benefits. The uncertainty will be addressed through scenarios and chance constraints, ensuring that SOC and power limits remain feasible most of the time.

ACKNOWLEDGMENT

The authors acknowledge Ho Chi Minh City University of Technology (HCMUT) and VNU-HCM for supporting this study.

REFERENCES

[1] A. R. Singh *et al*., "Electric vehicle charging technologies, infrastructure expansion, grid integration strategies, and their role in promoting sustainable e-mobility," *Alexandria Engineering Journal*, vol. 105, pp. 300–330, Oct. 2024, https://doi.org/10.1016/j.aej.2024.06.093.

[2] N. A. El-Taweel, H. Farag, M. F. Shaaban, and M. E. AlSharidah, "Optimization Model for EV Charging Stations With PV Farm Transactive Energy," *IEEE Transactions on Industrial Informatics*, vol. 18, no. 7, pp. 4608–4621, July 2022, https://doi.org/10.1109/TII.2021.3114276.

[3] K. Kouka, A. Masmoudi, A. Abdelkafi, and L. Krichen, "Dynamic energy management of an electric vehicle charging station using photovoltaic power," *Sustainable Energy, Grids and Networks*, vol. 24, Dec. 2020, Art. no. 100402, https://doi.org/10.1016/j.segan.2020.100402.

[4] R. Fachrizal, M. Shepero, M. Åberg, and J. Munkhammar, "Optimal PV-EV sizing at solar powered workplace charging stations with smart charging schemes considering self-consumption and self-sufficiency balance," *Applied Energy*, vol. 307, Feb. 2022, Art. no. 118139, https://doi.org/10.1016/j.apenergy.2021.118139.

[5] D. Chippada and M. D. Reddy, "Optimal planning of electric vehicle charging station along with multiple distributed generator units," *International Journal of Intelligent Systems and Applications*, vol. 14, no. 2, pp. 40–53, 2022, https://doi.org/10.5815/ijisa.2022.02.04.

[6] I. Chandra, N. K. Singh, P. Samuel, M. Bajaj, A. R. Singh, and I. Zaitsev, "Optimal scheduling of solar powered EV charging stations in a radial distribution system using opposition-based competitive swarm optimization," *Scientific Reports*, vol. 15, no. 1, 2025, Art. no. 4880, https://doi.org/10.1038/s41598-025-88758-y.

[7] S. Lai, J. Qiu, Y. Tao, and J. Zhao, "Pricing for Electric Vehicle Charging Stations Based on the Responsiveness of Demand," *IEEE Transactions on Smart Grid*, vol. 14, no. 1, pp. 530–544, Jan. 2023, https://doi.org/10.1109/TSG.2022.3188832.

[8] M. Çeçen, "Optimal integration of electric vehicle charging stations into a renewable-supported multi-energy system," *Electric Power Systems Research*, vol. 247, Oct. 2025, Art. no. 111832, https://doi.org/10.1016/j.epsr.2025.111832.

[9] S.-R. Jang, A.-Y. Yoon, and S.-S. Kim, "Optimal capacity determination of photovoltaic and energy storage systems for electric vehicle charging stations," *Journal of Energy Storage*, vol. 106, Jan. 2025, Art. no. 114730, https://doi.org/10.1016/j.est.2024.114730.

[10] X. Hu, H. Li, and C. Xie, "Optimal charging scheduling of an electric bus fleet with photovoltaic-storage-charging stations," *Applied Energy*, vol. 390, July 2025, Art. no. 125714, https://doi.org/10.1016/j.apenergy.2025.125714.

[11] A. R. A. Alphonse, A. P. P. G. Raj, and M. Arumugam, "Simultaneously allocating electric vehicle charging stations (EVCS) and photovoltaic (PV) energy resources in smart grid considering uncertainties: A hybrid technique," *International Journal of Energy Research*, vol. 46, no. 11, pp. 14855–14876, 2022, https://doi.org/10.1002/er.8187.

[12] K. Nareshkumar and D. Das, "Optimal location and sizing of electric vehicles charging stations and renewable sources in a coupled transportation-power distribution network," *Renewable and Sustainable Energy Reviews*, vol. 203, Oct. 2024, Art. no. 114767, https://doi.org/10.1016/j.rser.2024.114767.

[13] H. D. Nguyen, P. M. Le, and K. H. Truong, "Searching Optimal Placement and Operations of Energy Storage Systems based on Equilibrium Optimizer," *Engineering, Technology & Applied Science Research*, vol. 15, no. 4, pp. 24174–24180, Aug. 2025, https://doi.org/10.48084/etasr.11238.

[14] T. L. Duong and T. T. Nguyen, "Network Reconfiguration for an Electric Distribution System with Distributed Generators based on Symbiotic Organisms Search.," *Engineering, Technology & Applied Science Research*, vol. 9, no. 6, pp. 4925–4932, Dec. 2019, https://doi.org/10.48084/etasr.3166.